



## Universal response model for a corona charged aerosol detector

Joseph P. Hutchinson<sup>a,\*</sup>, Jianfeng Li<sup>a</sup>, William Farrell<sup>b</sup>, Elizabeth Groeber<sup>c</sup>, Roman Szucs<sup>d</sup>, Greg Dicoski<sup>a</sup>, Paul R. Haddad<sup>a</sup>

<sup>a</sup> Australian Centre for Research on Separation Science (ACROSS), School of Chemistry, Faculty of Science, Engineering and Technology, University of Tasmania, Private Bag 75, Hobart, Tas., 7001, Australia

<sup>b</sup> Pfizer Global R&D, La Jolla, CA, USA

<sup>c</sup> Pfizer Global R&D, Groton, CT, USA

<sup>d</sup> Pfizer Global R&D, Sandwich, Kent, CT13 9NJ, United Kingdom

### ARTICLE INFO

#### Article history:

Received 26 May 2010

Received in revised form 26 August 2010

Accepted 22 September 2010

Available online 29 September 2010

#### Keywords:

Universal detection  
Charged aerosol detector  
Corona  
Liquid chromatography  
UHPLC  
Model  
Response factor

### ABSTRACT

The universality of the response of the Corona Charged Aerosol Detector (CoronaCAD) has been investigated under flow-injection and gradient HPLC elution conditions. A three-dimensional model was developed which relates the CoronaCAD response to analyte concentration and the mobile phase composition used. The model was developed using the response of four probe analytes which displayed non-volatile behavior in the CoronaCAD and were soluble over a broad range of mobile phase compositions. The analyte concentrations ranged from 1 µg/mL to 1 mg/mL, and injection volumes corresponded to on-column amounts of 25 ng to 25 µg. Mobile phases used in the model were composed of 0–80% acetonitrile, mixed with complementary proportions of aqueous formic acid (0.1%, pH 2.6). An analyte set of 23 compounds possessing a wide range of physicochemical properties was selected for the purpose of evaluating the model. The predicted response was compared to the actual analyte response displayed by the detector and the efficacy of the model under flow-injection and gradient HPLC elution conditions was determined. The average error of the four analytes used to develop the model was 9.2% ( $n = 176$ ), while the errors under flow-injection and gradient HPLC elution conditions for the evaluation set of analytes were found to be 12.5% and 12.8%, respectively. Some analytes were excluded from the evaluation set due to considerations of volatility (boiling point <400 °C), charge and excessive retention on the column leading to elution outside the eluent range covered by the model. The two-part response model can be used to describe the relationship between response and analyte concentration and also to offer a correction for the non-linear detector response obtained with gradient HPLC for analytes which conform to the model, to provide insight into the factors affecting the CoronaCAD response for different analytes, and also as a means for accurately determining the concentration of unknown compounds when individual standards are not available for calibration.

© 2010 Elsevier B.V. All rights reserved.

### 1. Introduction

A significant problem posed within the pharmaceutical industry, and relevant to the entire discipline of liquid chromatography, is the desire to use a single detector which provides a uniform response for all compounds, regardless of their physicochemical properties. In the pharmaceutical industry, preliminary analysis is typically performed using photometric (UV/vis) detection, with successful drug candidates later being characterized by mass spectrometry (MS) and nuclear magnetic resonance (NMR) spectroscopy. However some pharmaceutical candidate molecules, as

well as synthetic intermediates and starting materials, do not contain UV/vis chromophores and require the use of a more universal detector. The ideal characteristics of such a detector are that all analyte types can be detected sensitively with uniform response factors on a single instrument, and the detector should be able to be used in conjunction with a wide variety of mobile phases/separation media for the purpose of achieving efficient separations. It is also advantageous for the detector to be of low cost. Uniform response factors remove the need for individual calibrants when determining the quantity of newly synthesized or unknown compounds.

Several detection techniques have been used in conjunction with HPLC including elemental detectors; optical detectors; such as; luminescence detectors; electrochemical detectors; nuclear magnetic resonance detectors; and mass spectrometric detectors [1,2]. Of these, mass spectrometry has been the universal detection system of choice due to its high sensitivity and the added mass

\* Corresponding author. Tel.: +61 3 6226 1072; fax: +61 3 6226 2858.  
E-mail addresses: [jhutchin@utas.edu.au](mailto:jhutchin@utas.edu.au), [Joseph.Hutchinson@utas.edu.au](mailto:Joseph.Hutchinson@utas.edu.au) (J.P. Hutchinson).

spectral information available [2,3]. However, it is not feasible to employ such expensive instrumentation for the routine screening of pharmaceuticals. Furthermore, mass spectrometers are known to suffer from variable response factors which can be attributed to the fact that a universal ionization interface is still being sought. Different ionization sources are suited to particular analytes and vary in their ability to ionize different compounds based on the chemical structure of the analyte and the surrounding ionization environment. In addition, LC–MS is less sensitive when used in scan mode to acquire spectral information.

Refractive index (RI) detectors offer an alternative choice for universal detection [4] but inherent problems are that many analytes give poor detection sensitivity and the use of gradient elution conditions usually results in a variable baseline. Another possibility is mass-specific chemiluminescence nitrogen detection, but limitations are that the compound of interest must contain nitrogen and the mobile phase must be kept free of nitrogen-containing components (which excludes the use of acetonitrile as the organic modifier in the HPLC eluent) [5,6]. A further class of detectors is the aerosol-based detectors. In these detectors, the HPLC column effluent is nebulized and then dried, producing analyte particles. This process accommodates a large variety of different compound classes provided they are less volatile than the mobile phase. These dried particles are then detected optically in the case of the evaporative light scattering detector (ELSD) [7] and the more sensitive condensation nucleation light scattering detector (CNLS) [8], or by charge transfer in the case of the Corona Charged Analyte Detector (CoronaCAD) [9]. ELSDs have been available for the last 20 years [7,10], but they have not been implemented widely due to their poor sensitivity in comparison to UV detectors when the analyte of interest absorbs strongly in the UV region, their limited dynamic range and non-linear response [11].

The CoronaCAD, first commercialized in 2004, passes a counter-current flow of gas over a high voltage corona wire which transfers a charge to particles and provides a response when the charged particles come into contact with a highly sensitive electrometer [12]. The CoronaCAD exhibits a wide dynamic range of approximately four orders of magnitude, ranging from low nanogram amounts on-column to amounts in the high micrograms. The detector response does not rely on the optical properties of analytes, nor on the ability of analytes to be ionized in the gas-phase [12] and is able to detect non-volatile analytes regardless of whether they contain a chromophore. However, like any aerosol detector, the CoronaCAD exhibits reduced response if the analyte is volatile or if particle formation is incomplete. However, the CoronaCAD is capable of detecting all non-volatile analytes, and most semi-volatile analytes with reduced response, and has been used in combination with a variety of different separation modes (isocratic and gradient reversed-phase, ion chromatography, hydrophilic interaction liquid chromatography, supercritical fluid chromatography, size exclusion chromatography) in normal and narrow-bore column formats, for a wide range of different analytes [12]. Applications utilising the CoronaCAD in the literature are quite diverse and include the analysis of synthetic polymers [13], inorganic ions [14], lipids [15], the determination of enantiomeric ratios [16], and for the analysis of pharmaceuticals [17–19] and their purity [20,21]. The CoronaCAD has been compared to other detectors, such as the ELSD, RI, UV and MS detectors, and has been found to be more sensitive and reproducible than the ELSD [19,22,23] and to exhibit more uniform response factors [13,16]. The RI detector exhibited poorer sensitivity than the CoronaCAD [13], while UV detection exhibited interference from some organic modifiers [24] and lower sensitivity for particular analytes [15,18], as well as non-uniform relative response factors [24]. Furthermore, the CoronaCAD is capable of detecting a greater range of analytes than the UV detector due to its ability to detect non-chromophoric compounds [25]. In com-

parison to MS, the CoronaCAD generally provided a more uniform analyte response than MS when electrospray ionization was used [20]. Pistorino and Pfeifer [26] compared the CoronaCAD to MS for the analysis of erythromycin and its precursor and found that the CoronaCAD was slightly more sensitive, exhibited better precision and also greater accuracy over the measured dynamic range. Hazotte et al. [27] further compared the CoronaCAD to a mass spectrometer with interchangeable APCI and ESI ionization sources and found that the CoronaCAD could universally detect all compounds of interest, while the MS required both ionization sources in order to detect all analytes. The CoronaCAD was 3–9 times more sensitive than the MS, and it was suggested that its use should be expanded due to its low cost, precision, wide dynamic range, and excellent measurement precision and accuracy.

A significant barrier to the implementation of the aerosol detectors has been that they exhibit non-linear calibration curves. The response of the CoronaCAD [9,12] and ELSD [27] have been described by the equation:

$$Y = Am^b \quad (1)$$

where  $Y$  is the output signal from the detector (peak area or height),  $m$  is the mass injected and  $A$  and  $b$  are constants ( $A$  represents the response intensity and  $b$  represents the response shape). The CoronaCAD has been found to give a lower response for particles greater than 10 nm in diameter and this explains the non-linear response at higher analyte concentration [9]. If linear calibration curves are desired, equation [1] can be converted to a linear relationship by taking the logarithm of both sides:

$$\log Y = b \log m + \log A \quad (2)$$

For aerosol detectors to gain wider acceptance, it is also necessary to overcome the “gradient effect” of these detectors. Organic modifier gradients are commonly used to achieve the desired chromatographic separation and this causes the composition of the mobile phase to differ for analytes which are eluted at different parts of the gradient. This in turn influences the nebulization and droplet evaporation processes in the detector and can lead to a 5–10-fold change in the response of an individual analyte due to variations in the transport efficiency of droplets/particles within the detector [28]. Efforts to mitigate this gradient effect have involved a gradient compensation approach whereby a second pump has been used to deliver a post-column inverse gradient prior to the aerosol detector [21,29]. This process ensured that the composition of the mobile phase entering the detector was constant. Another approach for overcoming the gradient effect is to construct a three-dimensional calibration plot, such as that performed by Matthews et al. [30] on an ELSD. Here, a single, non-retained compound was injected at regular intervals during gradient analysis to construct a three-dimensional calibration surface which accounted for response variation attributed to mobile phase composition and analyte concentration. The resultant calibration procedure could be performed on a variety of instrumentation and columns, however, each calibration was specific to these conditions was not individually transferable to other chromatographic systems involving different instrumentation and columns. Although the poor sensitivity of the ELSD was a limitation of this approach, the benefits of universal response allowed it to be incorporated successfully into in-house software [31] for high-throughput analyses of compounds in pharmaceutical discovery processes.

In the present study, a three-dimensional model relating detector response, analyte concentration and mobile phase composition has been developed on the CoronaCAD using the response of four probe non-volatile analytes under flow injection conditions. This response model was then evaluated using a series of analytes possessing a wide range of physicochemical properties to assess the uniformity of response of the detector. The efficacy of using this

response model for gradient separations was assessed by determining the concentration of further analytes eluted under gradient conditions.

## 2. Experimental

### 2.1. Instrumentation

A Dionex Rapid Separation Liquid Chromatograph (RSLC, Sunnyvale, CA) was used and consisted of a binary analytical pump with solvent selector, a 4-channel degasser, static mixer, in-line split-loop autosampler capable of injecting up to 100  $\mu\text{L}$ , a thermostatted column compartment, a variable wavelength detector and a Chromeleon Chromatography Data system. This system is capable of being used at pressures up to 11,603 psi and maintaining temperature within the range of 5–110 °C. A Corona Charged Aerosol Detector (CoronaCAD) was purchased from ESA Biosciences Inc. (Chelmsford, MA) and placed in-line after the UV–vis variable wavelength detector of the RSLC system. A refrigerated vapour trap (RVT4104) capable of chilling the gas waste from the CoronaCAD to –104 °C was purchased from Biolab Pty Ltd. (Scoresby, Australia). This was used to collect solvent vapours emitted from the CoronaCAD rather than allowing them to be released into the laboratory environment.

### 2.2. Materials

The mobile phase consisted of 0.1% formic acid in Milli-Q water (MilliPore Corporation, Milshiem, France), mixed with HPLC grade acetonitrile (Lichrosolv, Merck, Darmstadt, Germany). The mobile phase was degassed under vacuum and filtered through 47 mm Nylon filter membranes (0.2  $\mu\text{m}$  pore size, Grace Davison, Rowville, Australia) before use. All analyte standards were of analytical grade and purchased from Sigma–Aldrich (Sydney, Australia) or donated by Pfizer (La Jolla, CA). The 23 standards used in this study are given in Table 1, together with their chemical structures. Stock solutions of individual analytes were prepared at a concentration of 10 mg/mL in 0.1% formic acid, acetonitrile, or a 50:50 mixture of 0.1% formic acid and acetonitrile depending on solubility. Stock solutions were kept under refrigerated conditions for a maximum of 5 days. For chromatographic separations, mixed analyte working standards were prepared daily using the starting mobile phase as the solvent, or in dimethylsulfoxide (>99% purity, Merck, Darmstadt, Germany), depending on the solubility of the analytes. For chromatographic separations, the solvent used for standard preparation was not important as this is unretained on the column and elutes in the void before the analytes. Nitrogen gas created in-house from a nitrogen generator was used as the nebulizer gas for the CoronaCAD at a pressure of 35 psi.

### 2.3. Calculation of physicochemical properties

The physicochemical properties of the analytes used in this work were calculated using Advanced Chemistry Development (ACD/Labs) Physchem software (Version 12, Toronto, Canada). Based on the molecular structure of the analyte, the software predicted the log *P* value, log *D* value (at pH 2.6), *pK<sub>a</sub>*, molecular weight, boiling point, enthalpy of vaporization, polar surface area, refractive index, surface tension, molecular charge at pH 2.6, density and polarisability. The melting points of the analytes were obtained from the supplied material safety datasheets. Spartan'04 molecular modeling software (Wavefunction Inc., Irvine, CA) was used to optimize the geometrical configurations and calculate molecular volumes of the analytes used in this study. This was performed using the semi-empirical PM3 molecular orbital model. In addition, the four parameters used in the Kamlet–Taft linear solvation

energy relationship (LSER) model were calculated according to the empirical rules stipulated by Hickey and Passino-Reader [32]. These parameters were the intrinsic (van der Waal's) molecular volume, the dipole–dipole interactions and the hydrogen bond acidity and basicity of the analytes.

### 2.4. Response model development

Analyte response was measured at 44 different points in an experimental space spanning elution compositions containing 0–80% acetonitrile and a proportionate amount of aqueous mobile phase (0.1% formic acid in Milli-Q). Analyte concentrations ranged from 1  $\mu\text{g}/\text{mL}$  to 1 mg/mL (using an injection volume of 25  $\mu\text{L}$ ) which allowed all analytes to be detected within the dynamic range of the detector under all mobile phase compositions. Data were collected using mobile phase compositions at 0, 20, 50 and 80% acetonitrile, which provided the necessary precision and accuracy in the investigated concentration range with minimal number of experiments, and analyte concentrations of 0.001, 0.005, 0.01, 0.03, 0.06, 0.1, 0.2, 0.4, 0.6, 0.8, and 1 mg/mL. The response model was developed using the responses of sucralose, amitriptyline, dibucaine and quinine, all of which were soluble in all mobile phase compositions used in this study and exhibited non-volatile behavior in the CoronaCAD. Once the response of each analyte was known over the experimental space, the data were plotted as a 3D display using MATLAB software (The MathWorks, Natick, MA, USA) for visual verification and fitted to two 2nd order polynomial equations. The response model was then validated using the probe analytes under additional mobile phase compositions (10%, 30%, 40%, 60%, 70% acetonitrile) not used in the modeling process. The model was then further evaluated under flow-injection and gradient HPLC elution conditions using a further 19 analytes having a range of physicochemical properties. Once the associated error of the response model was known, it was possible to employ it to determine unknown analyte concentrations when the retention time (hence gradient composition) and detector response were known.

The detector response is dependent on analyte concentration and also the percentage of solvent in the mobile phase. Both relationships are non-linear and can be accurately described by polynomial regression with logarithm transformations of response and analyte concentration. Hence, a two-step model was developed to deal with both of these effects in a stepwise manner. The model starts by modeling detector response and analyte concentration for each compound while mobile phase concentration is kept constant and then linking the contribution of mobile phase concentrations into the model to describe the coefficients of the first step. The coefficients of each compound were averaged and fitted by polynomial models. The coefficients generated in the first step are directly related to response; the coefficients obtained in the second step describe the relation of solvent concentration with the coefficients calculated in the first step. In the fitness test, it is believed that stepwise fitnesses are simpler and easier to understand, more direct and suitable to the study therefore only two stepwise *r*<sup>2</sup> values are used to represent the fitness of the model.

### 2.5. Experimental procedures

#### 2.5.1. Flow injection analysis

The response model was developed under flow-injection conditions using the Dionex RSLC system without a chromatographic column in place. This dramatically reduced the time taken to develop the model and removed any chromatographic effects on the detector response since band widths of all analytes were identical under these conditions. The peak shape achieved under flow injection conditions exhibited a Gaussian distribution profile. To

**Table 1**  
The analytes chosen for use in this study.

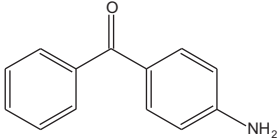
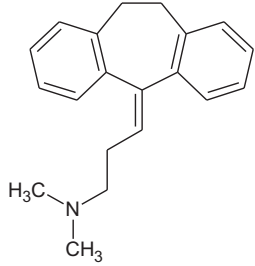
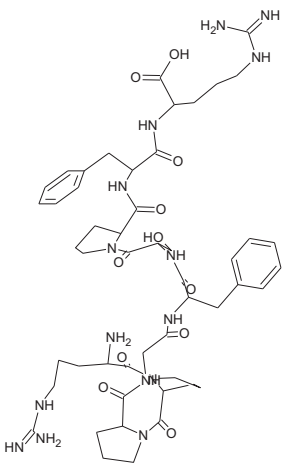
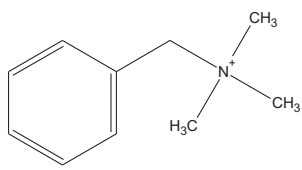
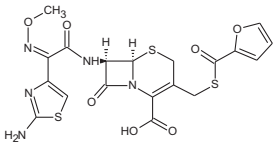
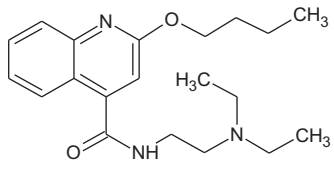
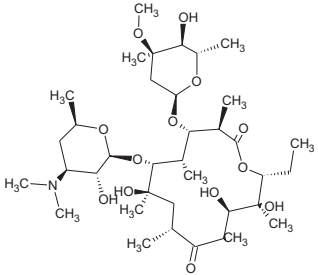
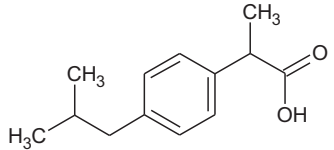
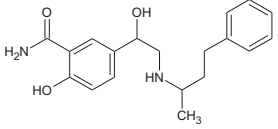
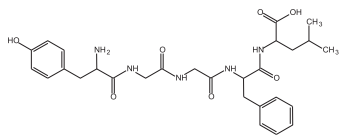
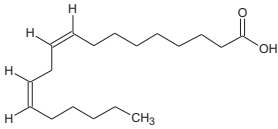
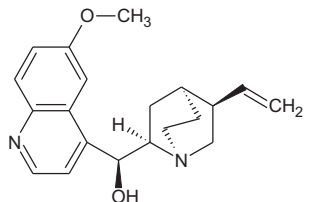
Analyte	Structure	Analyte	Structure
4-Aminobenzophenone		Amitriptyline	
Bradykinin		Benzyltrimethylammonium chloride	
Ceftiofur		Dibucaine	
Erythromycin		Ibuprofen	
Labetalol		Leucine-enkephalin	
Linoleic acid		Quinidine	

Table 1 (Continued)

Analyte	Structure	Analyte	Structure
Quinine		Sucralose	
Sucrose		Sphingomyelin	
Tetrabutylammonium bromide		Tetracaine	
Ticlopidine		Tocopherol	
Triphenylmethanol		Polysorbate 80	
Cyanocobalamin (Vitamin B12)			

ensure that the analyte band reaching the detector was uniform under flow-injection conditions, the samples were prepared in the same mobile phase composition as was generated by the pump. The sample injection volume was 25  $\mu\text{L}$  and the flow-rate was 1 mL/min to the detector. These experimental conditions were also used to assess the fit of the remaining 19 analytes to the model under flow-injection conditions at analyte concentrations of 0.01 mg/mL and a mobile phase composition of 50:50 acetonitrile:aqueous formic acid (0.1%). The CoronaCAD was set to its broadest range of 500 pA to ensure that the analyte response remained in scale over the entire experimental space.

### 2.5.2. Gradient elution analysis

The model was also evaluated under gradient elution conditions using a Dionex PolarAdvantage II separator column (3  $\mu\text{m}$  particle size, 3 mm diameter and 75 mm length). The polar-embedded nature of this stationary phase allowed a linear gradient from 0 to 100% acetonitrile and 100 to 0% aqueous formic acid (0.1%) to be used. The linear gradient reached 100% acetonitrile in 5 min and the mobile phase composition was then held constant for 3 min to ensure all analytes had eluted from the column. The injection volume was 25  $\mu\text{L}$  and a flow-rate of 1 mL/min was used. The CoronaCAD was set to the 500 pA range.

### 3. Results and discussion

#### 3.1. Requirements of universal detection

The goal of this study was to establish a detection system for gradient elution conditions in RPLC which could be used for a very wide range of analytes. Such a detection system is particularly important when standards are unavailable for calibration purposes. This case presents itself on numerous occasions in the pharmaceutical industry when quantifying unknown impurities, metabolites of active compounds or unknown compounds in the area of drug discovery. It is desirable that all analyte types will produce a response in the detector and ideally all analytes should have identical response factors. A further objective was to achieve universal detection over a wide dynamic range but also to provide adequate sensitivity for trace analysis.

The CoronaCAD exhibits many of the attributes of a universal detector for non-volatile compounds. It has been shown to provide uniform relative response factors under isocratic conditions, regardless of differences in the physicochemical properties of the analytes themselves [13,16,20,33]. However, under gradient elution conditions this uniform response is lost due to changes in droplet size distributions during nebulization and different evaporation rates causing changes in transport efficiency within the detector resulting from differing proportions of organic solvent in the mobile phase [28]. This does not necessarily pose a problem if a calibration standard exists for each analyte. However, if standards are unavailable, then the change in detector response with changing eluent composition must be overcome. A suitable approach to correct for the gradient effect in the detector is to develop an empirical model which relates mobile phase composition, analyte concentration and detector response. As the CoronaCAD has been shown to exhibit uniform response factors regardless of the analyte structure [33] for non-volatile analytes, it follows that all non-volatile analytes should exhibit a similar gradient response in the detector.

#### 3.2. Choice of analytes

Consideration of the physicochemical properties of analytes played an important part of the selection process of the analyte set. The goal of this work was not just to choose analytes that are known exhibit a uniform response on the CoronaCAD, but to investigate analytes of varying physicochemical properties so a true and fair view of the performance of the CoronaCAD could be formed. To demonstrate that the model developed is capable of being applied to a wide range of compounds, a set of 23 analytes was chosen to encompass a number of important physicochemical properties. The solubility of the analytes in the range of solvents used in this study was also considered in choosing the final analyte set. The chosen analytes are shown in Table 1.

The physicochemical properties considered were  $\log P$ ,  $\log D$  (at pH 2.6), melting point,  $pK_a$ , molecular weight, boiling point, enthalpy of evaporation, molecular charge at pH 2.6, molecular volume, charge density, polar surface area (PSA), refractive index, surface tension, density and polarisability. The Kamlet–Taft linear solvation energy relationship (LSER) model predicts chemical properties based upon molecular structure and the energy required to surround the solute with solvent molecules [32] and these parameters were also included due to the relevance of solvation during the nebulization and evaporation steps in the CoronaCAD detector. Four solvatochromic parameters are used in the LSER model, namely the intrinsic (van der Waals) molecular volume, the dipole–dipole interactions, the hydrogen bond acidity and hydrogen bond basicity.

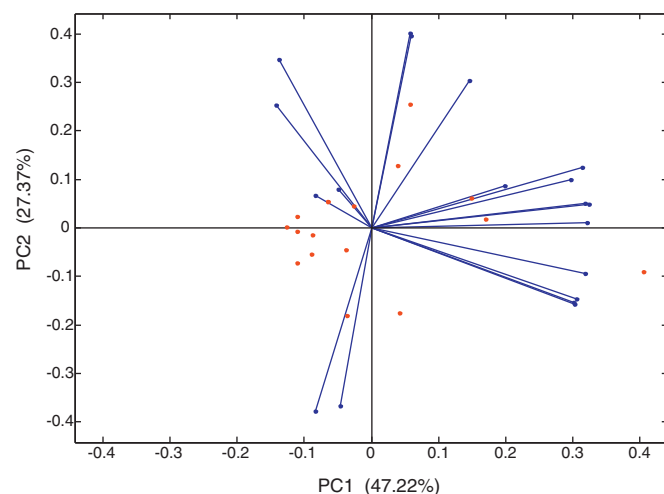


**Fig. 1.** Principal component analysis (PCA) bi-plot showing the spread of analytes over the chosen physicochemical properties. Each physicochemical property is represented as a vector in the 2D space.

It is difficult to identify a set of analytes which span equally all physicochemical parameters and selection of an analyte based on a particular physicochemical property often causes outliers to occur in others. Hence, the final analyte set represents the best compromise of the parameters chosen in this study. Fig. 1 provides a principal component analysis bi-plot where all of the physicochemical parameters are represented as vectors in a two-dimensional space and the analytes are represented by dots. Ideally, these vectors will be spread evenly without overlap and there would be no clustering of analytes. It is noted that vectors representing related physicochemical properties, such as boiling point and enthalpy of evaporation, are closely associated. The analytes chosen were found to provide a reasonable spread indicating adequate coverage of the designated physicochemical space.

#### 3.3. Empirical response model

The uniform analyte response of the CoronaCAD under isocratic conditions provides a basis for a universal model which takes into account the changing percentage of organic solvent in the mobile phase. When performing an analysis, knowledge of the elution time and the shape of the gradient applied allows the composition of the mobile phase in which the analyte enters the detector to be determined. Similarly, the response from the detector can be measured and these parameters can be used to construct a three-dimensional model to calculate the concentration of an unknown compound, based on the assumption that all analytes will exhibit a similar response.

The empirical model relating detector response to the mobile phase composition and analyte concentration was developed under flow-injection conditions with the column removed from the flow-path. This dramatically shortened the time required to acquire the necessary data points for the model and generated a response model specific to the detector, which removed chromatographic variation from the modeling process. The rationale of this approach was that the developed model could then be transferred to a variety of different chromatographic columns using a peak width correction factor which can be ascertained by a single run, rather than having to develop the whole model again for a different chromatographic column. The benefit of using linear gradient elution is that in theory, the peak widths of all analytes should be equal and hence differences between the peak shapes obtained under flow injection conditions and those obtained when performing chromatographic separations can be corrected by a single correction factor experi-

**Table 2**  
The coefficients of the CoronaCAD empirical model.

	$Q_{i,1}$	$Q_{i,2}$	$Q_{i,3}$
$P_{ACN,1}$	0.00001	-0.0006	-0.0778
$P_{ACN,2}$	0.00002	-0.0022	0.5499
$P_{ACN,3}$	-0.00017	0.0209	1.4041

mentally obtained in a single run. If the model had to be generated whenever a new column is used or the current column shifts in its retention, then the model becomes less useful in a practical sense.

The model was developed using four analytes exhibiting a non-volatile response in the CoronaCAD, as detailed previously. The model aimed to span mobile phase compositions ranging from 0 to 100% acetonitrile and to include the entire dynamic range of the detector. However, in practice the range of mobile phase compositions used in the model was restricted to 0 to 80% acetonitrile due to a sharp deviation in the detector response above these concentrations. The shape of the gradient response for the four probe analytes at constant analyte concentration is shown in Fig. 2(a) and the calibration curves for these analytes under isocratic conditions are shown in Fig. 2(b). Although the dynamic range of the detector spans 4 orders of magnitude, the response model was developed over the concentration range of 1  $\mu\text{g}/\text{mL}$  to 1  $\text{mg}/\text{mL}$  (using a 25  $\mu\text{L}$  injection volume) to ensure that a response was obtained under all eluent compositions, giving an on-column mass range of 25  $\text{ng}$  to 25  $\mu\text{g}$ . The detection limit under optimized conditions was approximately 0.02  $\mu\text{g}/\text{mL}$  using a mobile phase containing 70% acetonitrile and a S/N ratio of 3. Although there were small differences in their relative response factors the overall trends were similar for the four analytes shown in Fig. 2.

The empirical response model is a two-step model described by two 2nd order polynomial equations; one relating detector response indirectly to the percentage of acetonitrile (Eq. (3)), which in turn generated constants to be used in Eq. (4) which described the relation of the logarithms of the analyte concentration and the observed detector response.

The equations used to generate the model are:

$$P_{ACN,i} = Q_{i,1} \times [\text{ACN}]^2 + Q_{i,2} \times [\text{ACN}] + Q_{i,3}, \quad i = 1, 2, 3 \quad (3)$$

$$\text{Log(CoronaCAD response)} = P_{ACN,1} \times \log[\text{Analyte}]^2 + P_{ACN,2} \times \log[\text{Analyte}] + P_{ACN,3} \quad (4)$$

where [ACN] is the percentage of acetonitrile used in the eluent; [Analyte] is the concentration of analyte;  $Q_{ij}$  ( $i = 1, 2, 3, j = 1, 2, 3$ ) are the regression coefficients shown in Eq. (3); and  $P_{ACN,i}$  ( $i = 1, 2, 3$ ) are the coefficients shown in Eq. (4).

Table 2 provides the regression coefficients for the model and the correlation coefficients ( $r^2$ ) for Eqs. (3) and (4) were found to be 0.9995 and 0.9993, respectively. It should be noted that the first coefficient of  $P_{ACN,1}$  and  $P_{ACN,2}$  are arguably statistically insignificant as the logarithmic relationship between analyte concentration and response was almost linear. However, as the model was better described by a polynomial even just marginally, these values have been included to highlight the polynomial approach used in the modeling process to showcase the flexibility of the modeling procedure.

The error of the response model was assessed by comparing the measured analyte response with that calculated using the proposed model at each data point and averaging these errors for each analyte. The resultant errors are provided in Table 3 and the average error across all four analytes was 9.2%. The three-dimensional relationship between the parameters in the model is shown in Fig. 3.

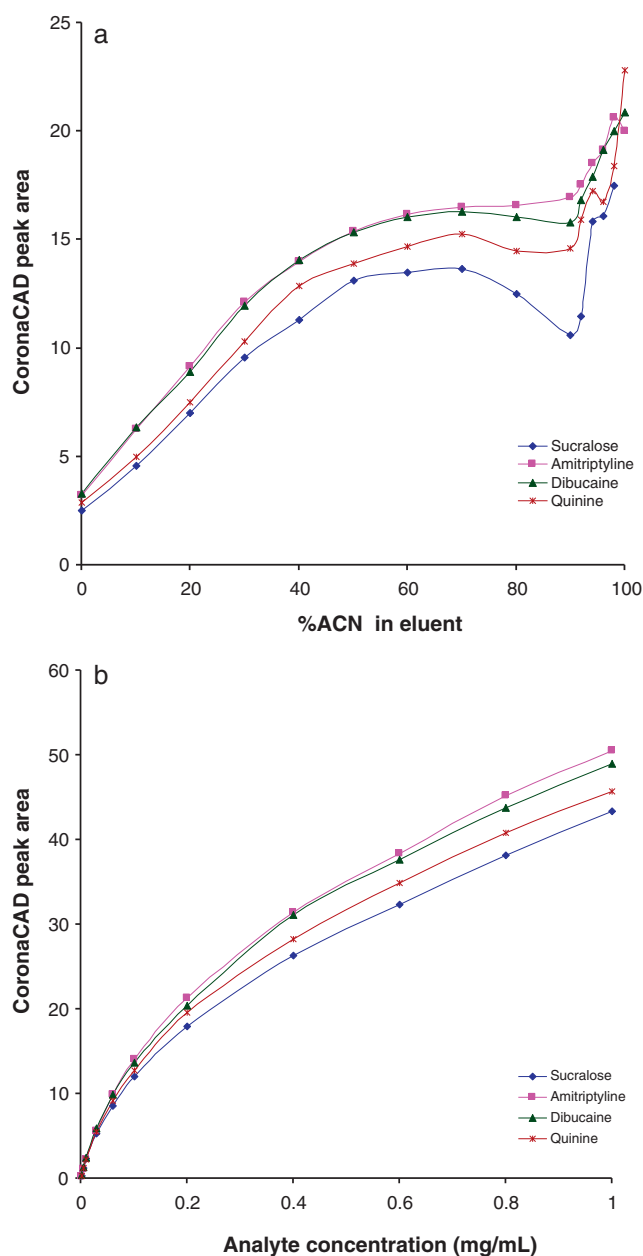


**Fig. 2.** (a) The gradient response of the CoronaCAD detector with changing eluent composition for four analytes used in the empirical model. *Conditions:* Flow injection analysis spanning mobile phase compositions of 0–100% acetonitrile mixed with formic acid (0.1% in Milli-Q). All analytes were prepared in same composition of mobile phase used for analysis at a concentration of 0.1  $\text{mg}/\text{mL}$  and a 25  $\mu\text{L}$  injection was performed. The flow rate used was 1  $\text{mL}/\text{min}$  and the measurements were performed with the CoronaCAD set on its broadest range of 500 pA. (b) The analyte concentration response of the CoronaCAD detector for four analytes used in the empirical model. *Conditions:* Flow injection analysis spanning analyte concentrations ranging from 1  $\mu\text{g}/\text{mL}$  to 1  $\text{mg}/\text{mL}$ . All analytes were prepared in mobile phase which was kept at a constant composition of 50% acetonitrile and 50% aqueous formic acid (0.1%). A 25  $\mu\text{L}$  injection was performed. The flow rate used was 1  $\text{mL}/\text{min}$  and the measurements were performed with the CoronaCAD set on its broadest range of 500 pA.

This clearly shows the non-linear analyte concentration response and the non-linear gradient effect which can result in a 5-fold increase in the detector response for a given concentration of analyte. The response surface also shows that the optimized response is achieved using a mobile phase containing 70% acetonitrile and this composition should be used for applications requiring maximum sensitivity.

**Table 3**

The comparison of the average relative error (calculated using absolute values) between the actual detector response measured and the response calculated using the CoronaCAD empirical model ( $n = 176$ ).

	Sucralose	Quinine	Amitriptyline	Dibucaine	Average of four analytes
Average relative error	9.3%	5.9%	11.4%	10.2%	9.2%

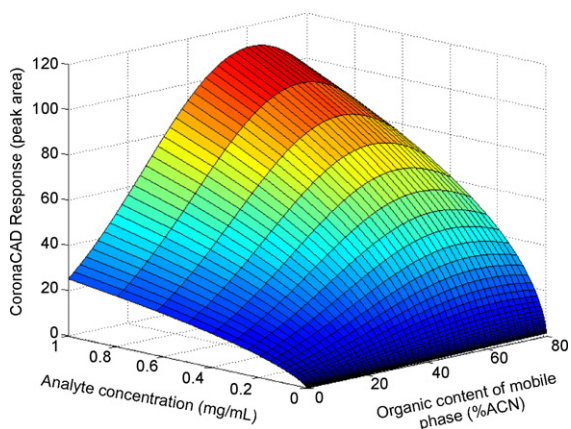


**Fig. 3.** The three-dimensional relationship found for four analytes relating the detector response, analyte concentration and the composition of the mobile phase.

### 3.3.1. Prediction of analyte concentration using the response model

The response model was tested using the remaining analytes initially selected under isocratic flow-injection conditions at the mid-point of the experimental space. Table 4 shows the difference between the actual and predicted analyte responses using the model under constant mobile phase conditions. From Table 4, it is evident that 5 of the 23 compounds exhibited large negative discrepancies between the actual and predicted responses. All of these analytes had relatively high volatility, resulting in a portion of the analyte being lost during the nebulization and evaporation steps in the detector. This effect is evident from Fig. 4 which shows the correlation between the relative error and the boiling point.

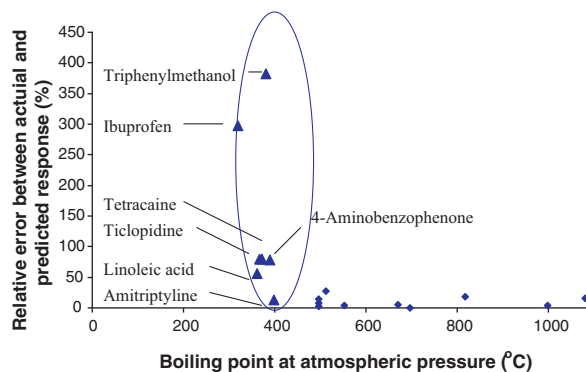


**Fig. 4.** Relationship between the error in the predicted response and the boiling point of the analytes. Conditions: Conditions used were as stated in Fig. 3(b) except the analyte concentration was kept constant at 0.01 mg/mL. The boiling points of the analytes were predicted using ACD/Labs Physchem software.

When analytes possessing boiling points below 400 °C (at atmospheric pressure) are excluded, this accounts for all of the outliers in Table 4. The boiling point of an analyte can be calculated *in silico* using ACD/Labs (Toronto, Canada) software or can be measured experimentally prior to analysis. Of interest in Fig. 5 are tetracaine and amitriptyline which exhibited satisfactory error values but had boiling points below the cut-off of 400 °C. This may be attributed to their possession of a tertiary amine functional group which is protonated under the experimental conditions used, while the boiling point calculations were performed on an uncharged molecule. The added hydrogen bonding effects may increase the effective boiling point of these analytes such that they do not evaporate significantly in the CoronaCAD. Once the outliers in Table 4 were removed, the

**Table 4**

Error between actual and predicted analyte response in the CoronaCAD. Conditions: Flow-injection analysis using a mobile phase containing 50% acetonitrile and 50% formic acid (0.1% in Milli-Q). Analyte concentration was kept constant at 0.01 mg/mL. Other conditions as stated in Fig. 3(b).

Analyte	Relative error between actual and predicted response	Outliers <sup>a</sup>	Absolute relative error
Sucralose	-5.2%		5.20%
Quinine	-8.4%		8.4%
Amitriptyline	-12.6%		12.6%
Dibucaine	-2.3%		2.3%
Ticlopidine	-79.6%	-79.6%	
Labetalol	3.9%		3.9%
Vitamin B12	-11.4%		11.4%
Tocopherol	-27.5%		27.5%
Tetrabutylammonium bromide	20.4%		20.4%
Triphenylmethanol	-382.0%	-382.0%	
Ibuprofen	-297.2%	-297.2%	
Bradykinin	-17.9%		17.9%
Quinidine	14.0%		14.0%
Tween80	-4.1%		4.1%
Tetracaine	-15.5%		15.5%
4-Aminobenzophenone	-78.3%	-78.3%	
Ceftiofur	-3.0%		3.0%
Erythromycin	17.6%		17.6%
Sucrose	-0.2%		0.2%
Leucine-enkephalin	-4.5%		4.5%
Sphingomyelin	20.6%		20.6%
Benzyltrimethylammonium chloride	36.0%		36.0%
Linoleic acid	-43.6%	-43.6%	
			Average absolute relative error 12.5%

<sup>a</sup> Defined as analytes exhibiting relative errors of magnitude greater than 40%.



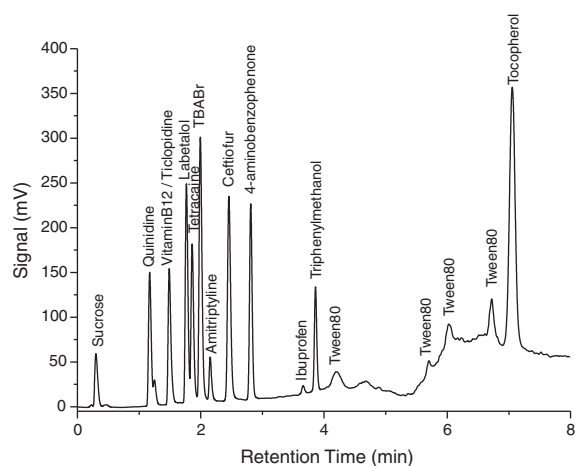


**Fig. 5.** A typical gradient separation of 14 analytes performed on the CoronaCAD detector. *Conditions:* Gradient: A linear gradient of 0–100% acetonitrile was mixed with aqueous formic acid (0.1%) over the time interval 0–5 min. Pure acetonitrile was held constant at 100% acetonitrile for 3 min. The flow rate was 1 mL/min. Injection: a 25  $\mu$ L injection of a 0.1 mg/mL mixed sample of 14 analytes prepared in DMSO was performed. The analytes were sucrose, quinidine, Vitamin B12, ticlopidine, labetalol, tetracaine, tetrabutylammonium bromide (TBABr), amitriptyline, ceftiofur, 4-aminobenzophenone, ibuprofen, triphenylmethanol, Tween80 and tocopherol. Column: A Dionex PolarAdvantage II column was used (3  $\mu$ m particles, 3.0 mm  $\times$  75 mm). Detection: The CoronaCAD detector was set to its broadest range of 500 pA.

overall relative error for 18 of the 23 compounds was 12.5%, which is acceptable given the wide variety in structures and physicochemical properties of the analytes studied.

The next step in the process was to determine if the model could be used under gradient elution conditions with a separation column in place. A fundamental difference between these conditions and the experimental conditions under which the model was created is the width of the analyte band that enters the detector. When a chromatographic column was used, the peak width was approximately 2.5 times greater than in the flow-injection mode. This leads to a dilution effect of the analyte. A benefit of using a linear solvent gradient is that the peak widths of all analytes across the gradient are theoretically the same [34]. Hence, although there is a distortion of

the analyte band reaching the detector, this effect is the same for all analytes across the gradient and can be accounted for using a single correction factor. This correction factor was found to be 1.533 and is specific to the particular column used, although negligible variation in the correction factor was observed when another column of different length and particle size was investigated. The benefit of this approach is that the model is not specifically created for one column and can be applied to a range of separation columns by simply calculating the peak broadening effect of one analyte relative to that measured in the model.

Table 5 shows the actual measured response of 16 analytes (after volatile analytes had been excluded, together with sphingomyelin which was not eluted under the gradient conditions used) on the CoronaCAD and the predicted response under gradient elution conditions. It was found that for the 16 analytes spanning a wide range of physicochemical properties, the associated error between the actual response and that predicted by the model was 49.7%. High errors were associated with four analytes: the two alkylammonium compounds, Polysorbate 80, and tocopherol. These analytes all had specific characteristics that distinguished them from other analytes in the test set. The two alkylammonium compounds were permanently charged, while tocopherol and Polysorbate 80 were eluted in a mobile phase composition which fell outside the modelled gradient conditions (0–80% acetonitrile). The quaternary ammonium compounds exhibited a much greater response than predicted by the model and it is clear that these compounds do not follow the same response pattern as for the compounds used to construct the model. When these four compounds were excluded, the overall error of the remaining 12 analytes was 12.8%. Given that such a diverse range of chemical compounds was evaluated in this study, the ability to quantify the majority of these with only 13% error on the CoronaCAD provides a means for the universal estimation of unknown components. To put this into perspective, without using the model the error would have been as large as 500%. The observed error in the CoronaCAD response model is significantly less than the 20% error associated with a similar response model on an ELSD detector [31] and the CoronaCAD also provides a 10-fold increase in detection sensitivity over the ELSD detector.

A typical gradient elution separation with CoronaCAD detection is shown in Fig. 5. This was performed on a polar-embedded,

**Table 5**  
Error between the actual response and the predicted response for 16 non-volatile analytes in the CoronaCAD under gradient elution conditions with a separation column in-line. *Conditions:* Gradient separations were performed as stated in Fig. 5, however, the concentration of analytes injected was 0.01 mg/mL in this case.

Analyte	Elution point in gradient (% ACN)	Actual conc. injected (mg/mL)	Predicted conc. using peak width correction of 1.533 (mg/mL)	Relative error between actual and predicted conc. (magnitude, %)	Relative error between actual and predicted conc. (magnitude, %)
Benzyltrimethylammonium chloride	0	0.0100	0.0297	197.0	<sup>a</sup>
Quinine	8.8	0.0100	0.0096	3.7	
Sucralose	16.5	0.0100	0.0093	6.9	
Labetalol	19.1	0.0100	0.0113	12.9	
Dibucaine	26.0	0.0100	0.0098	2.3	
Tocopherol	100.0	0.0100	0.0232	132.1	<sup>b</sup>
Vitamin B12	15.1	0.0100	0.0113	13.3	
Tetrabutylammonium bromide	21.4	0.0100	0.0160	60.3	<sup>a</sup>
Bradykinin	10.5	0.0100	0.0084	16.0	
Quinidine	7.6	0.0100	0.0127	27.4	
Tween80 (polymer)	Several	0.0100	0.0022	77.9	<sup>c</sup>
Tetracaine	20.2	0.0100	0.0075	24.9	
Ceftiofur	33.5	0.0100	0.0113	12.8	
Erythromycin	26.4	0.0100	0.0098	1.6	
Sucrose	0	0.0100	0.0083	16.9	
Leucine-enkephalin	18.7	0.0100	0.0114	14.2	
				Average 49.7%	Average 12.8%

<sup>a</sup> Permanently charged quaternary ammonium ions were omitted due to observed increased response in detector.

<sup>b</sup> Eluted in 100% acetonitrile mobile phase which is outside the scope of the model.

<sup>c</sup> Polymer exhibiting many small peaks making it difficult to quantitate on the CoronaCAD.

reversed-phase column which can be operated under a variety of mobile phase conditions ranging from 0 to 100% organic modifier. This allows polar analytes to be separated at the beginning of the gradient which cannot normally be accomplished on reversed-phase columns because of the requirement for a small amount of organic solvent to wet the hydrophobic functional groups. It was not the intention of this work to completely separate all of the test analytes, and this is evident in Fig. 5 where some of the analytes have co-eluted. The purpose of the gradient separation was to assess the response of analytes at differing positions along the linear solvent gradient and to see how well this correlated with the predicted response. Analytes that co-eluted were run separately to determine their detector response. It is evident from Fig. 5 that the volatile analytes (e.g. ibuprofen and triphenylmethanol) in the sample gave significantly reduced responses in the CoronaCAD.

#### 4. Conclusions

Universal and sensitive detection of analytes, irrespective of whether they contain a UV chromophore, has been a goal of separation science for some time. Aerosol-based detectors provide a viable approach and of these detectors, the CoronaCAD is known to exhibit uniform relative response factors under isocratic conditions for a wide range of non-volatile analytes and is more sensitive than evaporative light scattering detectors. However, the use of this detector has been restricted due to the variable response observed under gradient elution conditions.

In this work, the gradient effect has been modelled for analytes possessing a wide range of physicochemical properties on the CoronaCAD over a gradient elution profile spanning 0–80% acetonitrile. The resultant three-dimensional model relates detector response, analyte concentration and the mobile phase composition, allowing the CoronaCAD to be used for quantifying unknown compounds with acceptable error where individual calibrants are not available. This approach is applicable to non-volatile (boiling point >400 °C), neutral analytes which are eluted from the column under mobile phase compositions with <80% acetonitrile. This work has also highlighted the limitations of the aerosol-based detectors such as their non-uniform response for volatile compounds and therefore do not represent the solution to the search for a truly universal detector. However, these detectors are uniform in their response and suitable for most non-volatile compounds or can be used to complement existing detector technology.

Future work will assess the feasibility of using methanol as the organic modifier and identification of further physicochemical analyte properties which are critical to the performance of the detector.

#### Acknowledgements

The authors would like to thank Ray Bemish and Russell Robins from Pfizer Corporation for useful discussions. Funding for this project from the Australian Research Council (Grant #LP0884030) is gratefully acknowledged.

#### References

- [1] J. Cazes, Encyclopedia of Chromatography, Marcel Dekker Inc., New York, 2001.
- [2] M.P. Balogh, LC GC N. Am. 27 (2009) 130.
- [3] Y. Hsieh, E. Fukuda, J. Wingate, W.A. Korfmacher, Comb. Chem. High Throughput Screen. 9 (2006) 3.
- [4] B. Zhang, X. Li, B. Yan, Anal. Bioanal. Chem. 390 (2008) 299.
- [5] S. Ojanpera, I. Rasanen, J. Sistonen, A. Pelander, E. Vuori, I. Ojanpera, Ther. Drug Monit. 29 (2007) 423.
- [6] E.M. Fujinari, L.O. Courthaudon, J. Chromatogr. 592 (1992) 209.
- [7] L. Lucena, S. Cardenas, M. Valcarcel, Anal. Bioanal. Chem. 388 (2007) 1663.
- [8] J.A. Koropchak, C.L. Heenan, L.B. Allen, J. Chromatogr. A 736 (1996) 11.
- [9] R.W. Dixon, D.S. Peterson, Anal. Chem. 74 (2002) 2930.
- [10] N.C. Megoulas, M.A. Koupparis, Crit. Rev. Anal. Chem. 35 (2005) 301.
- [11] C.S. Young, J.W. Dolan, LC GC N. Am. 21 (2003) 120.
- [12] P.H. Gamache, R.S. McCarthy, S.M. Freeto, D.J. Asa, M.J. Woodcock, K. Laws, R.O. Cole, LC GC Eur. 18 (2005) 345.
- [13] D. Kou, G. Manius, S. Zhan, H.P. Chokshi, J. Chromatogr. A 1216 (2009) 5424.
- [14] Z. Huang, M.A. Richards, Y. Zha, R. Francis, R. Lozano, J. Ruan, J. Pharm. Biomed. Anal. 50 (2009) 809.
- [15] C. Schonherr, S. Touchene, G. Wilsner, R. Peschka-Suss, G. Francese, J. Chromatogr. A 1216 (2009) 781.
- [16] P. Wipf, S. Werner, L.A. Twining, C. Kendall, Chirality 19 (2007) 5.
- [17] C. Brunelli, T. Gorecki, Y. Zhao, P. Sandra, Anal. Chem. 2007 (2007) 2472.
- [18] L. Novakova, S.A. Lopez, D. Solichova, D. Satinsky, B. Kulichova, A. Horna, P. Solich, Talanta 78 (2009) 834.
- [19] N. Vervoort, D. Daemen, G. Torok, J. Chromatogr. A 1189 (2008) 92.
- [20] J. Reilly, B. Everatt, C. Aldcroft, J. Liq. Chromatogr. Relat. Technol. 31 (2008) 3132.
- [21] T. Gorecki, F. Lynen, R. Szucs, P. Sandra, Anal. Chem. 78 (2006) 3186.
- [22] K. Takahashi, S. Kinugasa, M. Senda, K. Kimizuka, K. Fukushima, T. Matsumoto, Y. Shibata, J. Christensen, J. Chromatogr. A 1193 (2008) 151.
- [23] R.G. Ramos, D. Libong, M. Rakotomanga, K. Gaudin, P.M. Loiseau, P. Chaminade, J. Chromatogr. A 1209 (2008) 88.
- [24] P. Sun, X. Wang, L. Alquier, C.A. Maryanoff, J. Chromatogr. A 1177 (2008) 87.
- [25] B. Forsatz, N.H. Snow, LC GC N. Am. 25 (2007) 960.
- [26] M. Pistorino, B.A. Pfeifer, Anal. Bioanal. Chem. 390 (2008) 1189.
- [27] A. Hazotte, D. Libong, M. Matoga, P. Chaminade, J. Chromatogr. A 1170 (2007) 52.
- [28] Z. Cobb, P. Shaw, L. Lloyd, N. Wrench, D. Barrett, J. Microcol. Sep. 13 (2001) 169.
- [29] A.d. Villiers, T. Gorecki, F. Lynen, R. Szucs, P. Sandra, J. Chromatogr. A 1161 (2007) 183.
- [30] B.T. Mathews, P.D. Higginson, R. Lyons, J.C. Mitchell, N.W. Sach, M.J. Snowden, M.R. Taylor, A.G. Wright, Chromatographia 60 (2004) 625.
- [31] A.W. Squibb, M.R. Taylor, B.L. Parnas, G. Williams, R. Girdler, P. Waghorn, A.G. Wright, F.S. Pullen, J. Chromatogr. A 1189 (2008) 101.
- [32] J.P. Hickey, D.R. Passino-Reader, Environ. Sci. Technol. 25 (1991) 1753.
- [33] ESA.Biosciences, Chelmsford, MA, USA, 2009.
- [34] P.R. Haddad, P.E. Jackson, Ion Chromatography—Principles and Applications, Elsevier Science, Amsterdam, 1990.